

more accurate formula is

$$\frac{d\sigma}{d\Omega} \Big|_{\eta^0 d} = \frac{1}{(4\pi)^2} \left[\left\langle \frac{w^2}{\epsilon_f \epsilon_f} \right\rangle_{av} \frac{E_i E_f}{W^2} \right] \frac{8}{3} |T^0|_{av}^2 \left(\frac{p^*}{k_{\gamma-d}^*} \right)^2 F^2(q^2)$$

(see Hadjioannou). The quantity in the bracket is ≈ 1 and for fixed p^* , $k_{\gamma-d}^* \approx k_{\gamma-p}^*$.

CROSS SECTION FOR $\pi^- p \rightarrow \Lambda K^0$: STRUCTURE NEAR Σ THRESHOLD*

O. Van Dyck, R. Blumenthal, S. Frankel, V. Highland,† J. Nagy,
T. Sloan,‡ M. Takats, W. Wales, and R. Werbeck

Department of Physics, University of Pennsylvania, Philadelphia, Pennsylvania 19104

(Received 9 June 1969)

The cross section for the reaction $\pi^- p \rightarrow \Lambda K^0$ has been measured at nine energies from 790 to 1060 MeV, with a beam resolution of $\pm 1\%$. The results indicate that a strong, narrow ($\Gamma \leq 20$ MeV) peak in the cross section lies within the energy bin centered at 893 MeV.

We have measured the threshold-region cross sections for the reaction $\pi^- p \rightarrow \Lambda K^0$ in a spark-chamber experiment carried out at the Princeton-Pennsylvania accelerator.

A diagram of the apparatus¹ appears in Fig. 1. A beam of negative pions, designed to give a nearly square energy window of 1% half-width, was focused on a 5-cm-long liquid-hydrogen target. An anticoincidence counter and a coincidence hodoscope were used after the target to detect the charged decays from the neutral strange particles. The spark-chamber tracks of the incident pions and the charged decay products were photographed in two 90° stereo views. Approximately 30% of the pictures show an apparent single vee, the majority being from the decay $\Lambda \rightarrow p\pi^-$.

The measurement of the pictures was fully automatic. The University of Pennsylvania Hough-Powell flying-spot digitizer processed the 200 000 pictures which were taken in the experiment. The resultant digitizings were processed by a computer program² which sought the single vee characteristic of the two-body charged decay of a neutral particle. The program found vee events with 90% efficiency.

Geometric criteria were applied to each event to test the hypothesis that the vee was a $\Lambda \rightarrow p\pi^-$ decay from ΛK^0 production. These criteria required that the reconstructed decay and production vertices were within the fiducial areas, that the decay geometry was compatible with a two-body decay, that stereo pairing by pattern was consistent with stereo pairing by digitizing density, and that the track with the smaller decay

angle, which was assumed to be the proton, was more heavily ionizing.

The kinematic reconstruction is singly constrained if all masses are assumed. The final selection of events was based on limits imposed on the reconstructed incident-pion energy T_R . Multiple scattering in the apparatus (~ 10 mrad) and inaccuracy in track fitting reduced the precision of this reconstruction. The full width at half-maximum height of the spectrum of T_R is 50 MeV. A consequence of this spread is that Λ 's from Σ^0 production and decay ($\pi^- p \rightarrow \Sigma^0 K^0$, $\Sigma^0 \rightarrow \Lambda \gamma$) cannot be accurately separated from Λ 's produced directly. In addition the Λ center-of-mass angle cannot be accurately reconstructed.

The Λ yield was defined as the product of the

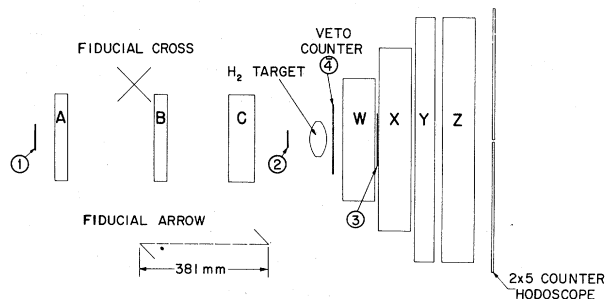


FIG. 1. Apparatus: 1-2 are the beam counters and ABC are spark chambers determining the incident pion line. Λ 's are produced in the 5-cm H_2 target and are required to decay between counters 4 and 3. The charged decay products are observed in spark chambers WXYZ. The hodoscope is a square array two counters high and five counters wide, in which any pair (2/10) were required for the Λ trigger. The complete counter trigger requirement was 1243(2/10).

number of triggers per incident pion and the number of Λ decays found per usable picture:

$$\text{Yield} = \frac{\text{Triggers}}{\text{Pion}} \frac{\Lambda\text{'s}}{\text{Usable picture}}.$$

(The track-finding program recorded as unusable the 10% to 20% of the pictures which had faulty or confusing beam tracks independent of the track pattern in the decay chambers.)

The center of the distribution of the reconstructed pion beam energy was about 12 MeV below the energy determined by a wire orbit of the beam-transport system. The average of these differences has been subtracted from the energy determined by wire orbit to give the beam energies specified in the data. This correction may introduce an error of about ± 5 MeV in the given energies.

Above the threshold for the reaction $\pi^-p \rightarrow \Sigma^0 K^0$ (903.6 MeV), the measured Λ yield includes the contribution from $\Sigma^0 \rightarrow \Lambda \gamma$ decays. The reconstruction assumed that all events come from decays of directly produced Λ 's, but the reconstructed pion energy, for events originating from Σ^0 decays, is lower by about 100 MeV than the true pion energy. The mixture of the two types of events gives the bimodal distribution of T_R shown in Fig. 2(a). A Monte Carlo simulation of events from the two sources was used to estimate the fraction of the observed yield from Σ^0 decays [see Fig. 2(b)].

The Λ yield as calculated above is shown in Fig. 3(a). The upper set of points is the total yield including $\Sigma \rightarrow \Lambda$. Typical points contain

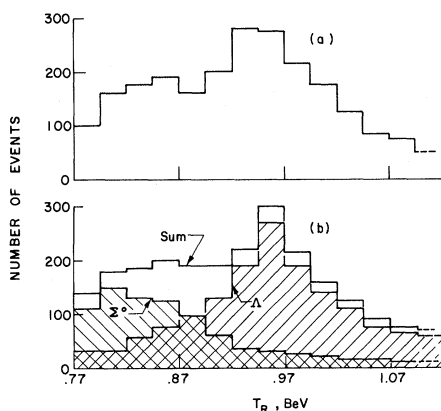


FIG. 2. (a) Distribution of reconstructed incident-pion energy T_R from real events created at 963 MeV. (b) Distribution of T_R from Monte Carlo events for $\pi^-p \rightarrow \Lambda K^0$ and $\pi^-p \rightarrow \Sigma^0 K^0, \Sigma^0 \rightarrow \Lambda \gamma$. The sum is shown and can be compared with the data in (a).

about 2000 events; the errors shown are statistical. The lower set has the $\Sigma \rightarrow \Lambda$ contribution subtracted; the larger errors on the lower points reflect the uncertainty in this correction.

The calculation of the cross section from the yield assumes a knowledge of the detection efficiency E_T of the system. The total detection efficiency E_T is defined as the product of the detection efficiency E for an isotropic distribution and a correction factor \bar{g} for the actual angular distribution: $E_T = E\bar{g}$. Since the experiment contained a considerable bias against Λ 's produced backward in the center of mass, the correction factor \bar{g} is needed to convert yields to cross sec-

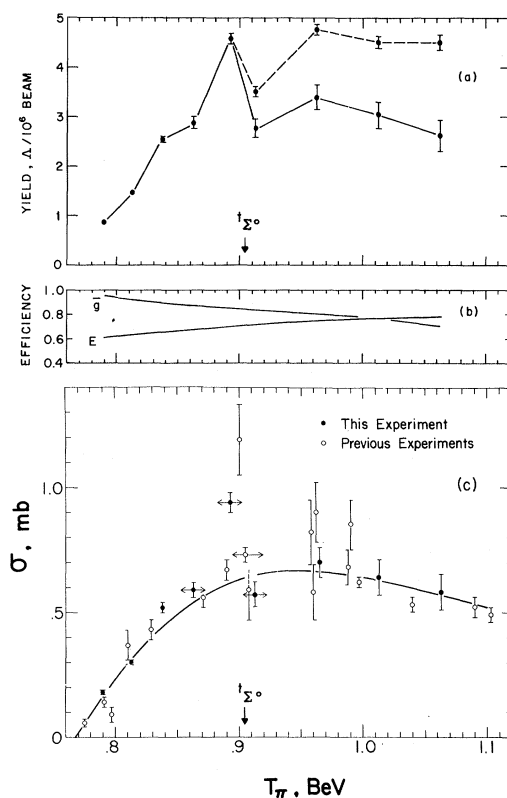


FIG. 3. (a) Observed yield of Λ . Above Σ^0 threshold ($\dagger \Sigma^0$), the upper points show the total yield including Λ 's from $\Sigma^0 \rightarrow \Lambda \gamma$, and the lower points show the yield with the estimated fraction of Σ events subtracted. (b) Detection efficiency E for isotropic ΛK production, and correction factor \bar{g} for actual production angular distribution obtained from bubble chamber data. E is on an arbitrary scale. The product efficiency $E\bar{g}$ is nearly flat over the energy range. (c) Production cross section for $\pi^-p \rightarrow \Lambda K^0$ from all experiments. The source of previous data may be identified in Rush, Ref. 3. The curve is given by the fit to the previous data by the Rush model. Near Σ threshold, some of the data points have horizontal arrows indicating the energy range in which σ has been averaged.

tions. Unfortunately, the reconstruction of the center-of-mass angle was not sufficiently reliable to allow a self-consistent correction. The angular variation in the cross section was determined from a compilation of bubble-chamber data,³ and \bar{g} was computed with Monte Carlo events using the "bias-matrix" technique.⁴ (A local variation in the actual production angular distribution such as may occur at 893 MeV would cause the computed correction factor \bar{g} to have a small error; for example, if $\langle \cos\theta_{\Lambda c.m.} \rangle$ changed by -0.1 , \bar{g} would change by -4% .) The factors E and \bar{g} are plotted in Fig. 3(b). The product is nearly flat over the whole energy range.

The corrected cross sections for ΛK production, $\sigma = \text{yield}/E_T$, in millibarns at (MeV), are

$$\begin{aligned}\sigma(790) &= 0.18 \pm 0.07, & \sigma(813) &= 0.30 \pm 0.01, \\ \sigma(838) &= 0.52 \pm 0.02, & \sigma(863) &= 0.59 \pm 0.03, \\ \sigma(893) &= 0.94 \pm 0.04, & \sigma(913) &= 0.57 \pm 0.06, \\ \sigma(963) &= 0.70 \pm 0.06, & \sigma(1013) &= 0.64 \pm 0.07, \\ \sigma(1063) &= 0.58 \pm 0.07.\end{aligned}$$

From a study of possible systematic errors, we assign an overall uncertainty of 8% to the normalization of the cross section over the whole energy range.

The most interesting feature of the data is the pronounced peak in the yield and cross section at 893 MeV. A comparison with previously reported results is shown in Fig. 3(c). This experiment is the first to measure the production cross section over this wide energy range. Away from Σ threshold, our data are generally in good agreement with previous data and the Rush³ fit shown in the figure. Given the energy bins covered and the possibility of a narrow peak, our cross section at 893 MeV may very well be consistent with an early bubble-chamber result,⁵ $\sigma(900 \text{ MeV}) = 1.19 \pm 0.14 \text{ mb}$, and a later result⁶ from the same laboratory, $\sigma(905 \text{ MeV}) = 0.73 \pm 0.03 \text{ mb}$. We cannot account for the discrepancy with Keren's measurement of $\sigma(890 \text{ MeV}) = 0.67 \pm 0.04 \text{ mb}$.

Whether this sharp peak is a manifestation of the cusp effect⁶⁻⁸ at Σ threshold, results from an unusually narrow resonance in the π^-p system,⁹ or has some other explanation must await more accurate experimental studies in this energy region.

We acknowledge with thanks the assistance given to us at the Princeton-Pennsylvania accelerator, at the New York University-Atomic Energy Commission Computing Center, and by the staff of the Pennsylvania Hough-Powell flying spot digitizer.

*Experimental work carried out at the Princeton-Pennsylvania Accelerator and supported in part by the U. S. Atomic Energy Commission.

†Now at Physics Department, Temple University, Philadelphia, Pa.

‡Now at Department of Physics, University of Lancaster, Bailrigg, Lancaster, England.

¹A more detailed description of the apparatus appears in S. Frankel, V. Highland, T. Sloan, W. Wales, and O. Van Dyck, Phys. Rev. **177**, 2113 (1969).

²O. Van Dyck, in Proceedings of the International Conference on Programming for Flying Spot Devices, Munich, Germany, 1967, edited by B. W. Powell and P. Seyboth (Max Planck Institute, Munich, Germany, 1967), p. 33.

³J. E. Rush, Jr., Phys. Rev. **173**, 1776 (1968).

⁴S. Frankel and O. Van Dyck, Princeton-Pennsylvania Accelerator Research Report No. PPAR 4, 1968 (unpublished).

⁵Reported by J. Steinberger, in Proceedings of the International Conference on High Energy Physics, Moscow, 1959 (Academy of Sciences, Moscow, U.S.S.R., 1960), p. 443.

⁶M. H. Alston, J. A. Anderson, P. G. Burke, D. D. Carmony, F. S. Crawford, N. Schmitz, and S. E. Wolf, in Proceedings of the Tenth International Conference on High Energy Physics, Rochester, New York, 1960, edited by E. C. G. Sudarshan, J. H. Tinlot, and A. C. Melissinos (Interscience Publishers, Inc., New York, 1960), p. 378; S. E. Wolf, N. Schmitz, L. J. Lloyd, W. Laskar, F. S. Crawford, J. Button, J. A. Anderson, and G. Alexander, Rev. Mod. Phys. **33**, 439 (1961); J. A. Anderson, F. S. Crawford, B. B. Crawford, R. L. Golden, L. J. Floyd, G. W. Meisner, and L. R. Price, in Proceedings of the International Conference on High Energy Physics, CERN, 1962, edited by J. Prentki (CERN Scientific Information Service, Geneva, Switzerland, 1962), p. 271.

⁷F. Eisler, P. Franzini, J. M. Gaillard, A. Garfinkel, J. Keren, R. Plano, A. Prodell, and M. Schwartz, Rev. Mod. Phys. **33**, 436 (1961); J. Keren, Phys. Rev. **133**, B457 (1964).

⁸R. K. Adair, Phys. Rev. **111**, 632 (1958).

⁹The narrow peak reported here in the ΛK partial cross section is not evident in the π^-p elastic cross section studied in detail by T. Bowen, W. R. Davies, Jr., D. A. DeLise, E. W. Jenkins, J. J. Jones, R. M. Kalbach, and E. Malamud, Phys. Rev. **178**, 2082 (1969).